Seasonal Climatic Effects and Feedbacks of Anthropogenic Heat Release due to Global Energy Consumption with CAM5

Bing Chen[1, 2, 3], C. Wu[2, 5], X. Liu[2*], Chen L.[4], Jian Wu[1], H. Yang[6], Tao Luo[7], Xue Wu[5], Yiquan Jiang[8], Lei Jiang[9], H. Y. Brown[2], Z. Lu[2], W. Fan[1], G. Lin[2], Bo Sun[9], M.Wu[2]

[1]Key Laboratory of Atmospheric Environment and processes in the Boundary Layer over the Low-latitude Plateau Region, Department of atmospheric science, Yunnan University, Kunming, 650091, China
[2]Department of Atmospheric Science, University of Wyoming, Laramie, WY 82071, USA
[3]Ministry of Education Key Laboratory for Earth System Modeling, Tsinghua University, Beijing100084, China
[4]The State Key Laboratory of Remote Sensing Science, Institute of Remote Sensing and Digital Earth, Chinese Academy of Sciences, Beijing 100101, China
[5] Institute of Atmospheric Physics, Chinese Academy of Sciences, Beijing 100029, China
[6]ICAS, School of Earth and Environment, University of Leeds, Leeds, LS2 9JTv, UK
[7]Hefei Institutes of Physical Science, Chinese Academy of Sciences, Hefei, Anhui, 230031, China
[8]CMA-NJU Joint Laboratory for Climate Prediction Studies, Institute for Climate and Global Change Research, School of Atmospheric Sciences, Nanjing University, Nanjing, China
[9]Nanjing University of Information Science and Technology, Nanjing 210044, China

Corresponding to: Prof. X. Liu, Department of Atmospheric Science, University of Wyoming, Laramie, WY 82071, USA. E-mail: xliu6@uwyo.edu.

Abstract

Anthropogenic Heat Release (AHR) is the heat generated in global energy consumption, which has not been considered in global climate models generally. The global high-resolution AHR from 1992 to 2013, which is estimated by using the Defense Meteorological Satellite Program (DMSP)/Operational Linescan System (OLS) satellite data, is implemented into the Community Atmosphere Model version 5 (CAM5). The seasonal climatic effects and possible feedbacks of AHR are examined in this study. The modeling results show that AHR increases the global annual mean surface temperature and land surface temperature by 0.02 ± 0.01 K(1σ uncertainty) and 0.05 ± 0.02 K(1σ uncertainty), respectively. The global climatic effect of AHR varies with season: with a stronger climatic effect in the boreal winter leading to global mean land surface temperature increases by 0.10 ± 0.01 K (1σ uncertainty). In the selected regions (40° N – 60° N, 0° E – 45° E) of Central and Western Europe the average surface temperature increases by 0.46 K in the boreal summer, and in the selected regions (45° N – 75° N, 30° E – 140° E) of northern Eurasia the average surface temperature increases by 0.83 K in the boreal winter. AHR changes the height and thermodynamic structure of the global planetary boundary layer, as well as the stability of the lower troposphere, which affects the global atmospheric circulation and low cloud fraction. In addition, at the surface both the shortwave radiation flux in the boreal summer and the down-welling longwave flux in the boreal winter change significantly, as a result of the change in low clouds caused by the effect of AHR. This study suggests a possible new mechanism of AHR effect on global climate through changing the global low-cloud fraction, which is crucial for global energy balance, by modifying the thermodynamic structure and stability of the lower troposphere. Thus this study improves our understanding of the global climate change caused by human activities.

Keywords: anthropogenic heat release, climatic effect, climate feedback, climate change

1. Introduction

Human activity is considered as the predominant cause for global warming since the mid-20th century (IPCC, 2013). Human activities have changed and continue to change the Earth's atmospheric composition, which will impact the energy balance of the Earth-atmosphere system (Hansen et al., 2005; IPCC, 2013). Various types of energy resources are consumed in the human society, all of which ultimately result in anthropogenic heat released into the atmosphere. According to the global energy consumption statistics, the current global mean flux of AHR is approximately 0.03 W m^{-2}, compared to the total radiative forcing (RF) by human activities approximately +2.29 [1.13~3.33] W m^{-2} (IPCC, 2013). However, in comparing AHR with other climatic forcing agents (e.g., greenhouse gases), the global spatial distribution of AHR has much stronger spatial and temporal variations: in populated urban regions (such as Tokyo) the flux of AHR may exceed 1000 W m^{-2} (Ichinose et al., 1999), whereas in deserted regions it is close to 0. The impact of AHR on climate in urban regions has increased significantly in the last 20 years due to the global urbanization and unbalanced economic development (Chen et al., 2014). While the regional climatic effect of AHR has received much attention in the previous research work (Oke, 1988; Ichinose et al., 1999; Block et al., 2004; Fan and Sailor, 2005; Block et al., 2004; Tong et al., 2004; Sailor and Lu, 2004; Fan and Sailor, 2005; IPCC, 2007; Lee et al., 2009; Chen et al., 2012; Chen and Shi, 2012; Lindberg et al., 2013; Wu and Yang, 2013; Yang et al., 2014; Wang et al., 2015; Dong, et al., 2017; Zhong et al., 2017), only a few studies investigated the potential global climatic effect of AHR (Flanner et al., 2009; Zhang et al., 2013; Chen et al., 2014). Previous research shows that AHR may be a missing forcing agent for the additional winter warming trends in observations over northern Asia and North America (Zhang et al., 2013), and it may have an impact on global atmospheric circulation (Chen et al., 2014). Flanner (2009) showed that significant increases in annual-mean temperature and planetary boundary layer (PBL) height occur over gridcells where the flux of AHR exceeds 3.0 W m^{-2}. Zhang et al. (2013) showed that AHR is probably a missing forcing for the additional winter warming trends in observations, leading as much as 1K in mid- and high latitudes in North America and Eurasia. Chen et al. (2014) showed that AHR is able to affect global atmospheric circulation, leading to 1-2 K increase in the high-latitude areas of Eurasia and North America.

While previous studies focus on the effect of AHR on temperature and general circulation, the understanding of the possible feedbacks and physical mechanisms of AHR on the global climate is still limited. The seasonal difference of AHR effects on global climate is still uncertain. Furthermore, the effects of AHR on the structure of PBL, clouds, and energy balance at the surface are not investigated. Considering accelerated urbanization (McCarthy et al., 2010) and rising energy demand in the future, the effect of AHR on global climate will become more pronounced. In this study, in order to explore seasonal variations of effects and feedbacks of AHR on multiple climate variables other than merely temperature, the high-resolution global distribution of AHR, which was estimated from remote sensing observations (Chen et al., 2014), is implemented into the global climate model Community Atmosphere

Model version 5 (CAM5) to examine the possible effect of AHR on the boundary layer structure, the stability of the lower troposphere, and associated climatic feedbacks. We will address the following questions in this study: what are the feedbacks to the lower tropospheric stability and boundary layer structure as a result of change in temperature induced by AHR? How are the low-level clouds changed, which can further affect the surface energy budget and thus surface temperature? What are the seasonal variabilities of AHR effects and climatic feedbacks?

The structure of this paper organized as follows. The descriptions of data, method and model experiments are given in Section 2. Section 3 analyzes the modeling results and discusses possible physical mechanisms for different seasonal climatic effect of AHR on global climate. Conclusions are drawn in Section 4, and discussion is listed in Section 5.

2. Data, method and model experiments

2.1 Data and method for estimating global distribution of AHR

The high-precision grid distribution of AHR on a large scale is crucial for climate models. Previous research on AHR focused on the regional estimation (Ichinose et al., 1999; Lee et al., 2009; Allen et al., 2011). In order to derive an accurate global high-resolution distribution of AHR, the National Oceanic and Atmospheric Administration (NOAA) Defense Meteorological Satellite Program (DMSP) Operational Linescan System (OLS) data (http://ngdc.noaa.gov/eog/dmsp/downloadV4composites.html) are used. Continuous stable light data from 1992 to 2013 are applied in this study to derive the global distribution of AHR as in Chen et al. (2014；2016). This method is based on the fact that DMSP/OLS data is consistent with local economy development levels and energy consumption statistics, which has been proven to very useful for estimating the global distribution of AHR (Chen et al., 2015). Figure 1 shows the global distribution of AHR, which is geographically concentrated, and is generally well correlated with the regional economic development levels (Chen et al., 2016). The global mean flux of AHR is 0.03 W m^{-2}, while the AHR fluxes in economically developed regions are much larger than the global mean. Europe, Eastern and Southern Asia, and North America are the three regions where the AHR is most concentrated, forming the heating centers in the global lower atmosphere. The developing process of AHR is apparent when looking at continuous estimation results by applying the DMSP/OLS data (Chen et al., 2014). Due to the unique ability to detect low levels of visible and near-infrared radiance at night, the DMSP/OLS data provides an effective way to estimate the large-scale high-resolution distribution of AHR (Chen et al., 2012; Chen et al., 2014).

2.2 Model and Experiments

In this study the grid-point data of the global distribution of AHR from 1992 to 2013 are applied in the CAM 5 model to study the effect of AHR on the global lower troposphere. CAM 5 (Neale et al. 2010) is the atmosphere component of the NCAR Community Earth System Model (CESM). It uses the finite volume methods in the dynamical core and a tracer transport algorithm. The large-scale cloud condensate and cloud fraction as well as the horizontal and vertical overlapping of clouds are treated by a cloud macrophysics scheme by Park et al. (2014). Stratiform microphysical processes are represented by a two-moment scheme (Morrison and Gettelman, 2008) as implemented by Gettleman et al. (2010). A modal aerosol model (MAM) by Liu et al. (2012) is coupled with the cloud microphysical scheme to represent the aerosol-cloud interactions through the droplet activation (Abdul-Razzak and Ghan, 2000) and ice nucleation/droplet freezing (Liu and Penner, 2005; Liu et al., 2007). The moist turbulence scheme is from Bretherton and Park (2009). Shallow convection is parameterized following Park and Bretherton (2009), and deep convection is treated following Zhang and McFarlane (1995) with further modifications by Richter and Rasch (2008). The radiation scheme has been updated to the Rapid Radiative Transfer Method for GCMs (RRTMG) by Iacono et al. (2008). More details of these schemes and parameterizations can be found in Neale et al. (2010). CAM5 is widely used in the research on climate variability and change (Hurrell et al., 2013).

In this study, CAM5 is run in the coupled land-atmosphere mode with prescribed monthly sea surface temperature and sea ice coverage (Hurrell et al., 2008), following the Atmospheric Model Intercomparison Project (AMIP) protocols (Gates, 1992). The model simulations with the same setup as used in this study have been evaluated against various observations (Bacmeister et al., 2014). These results show that CAM5 can reasonably simulate the observed climate states and variabilities. The horizontal resolution in our model experiments is 1.9°×2.5° with 30 vertical levels, and the time step is 30 minutes. Historical greenhouse gas concentrations, and anthropogenic aerosol and precursor gas emissions are prescribed as in Kay et al. (2015). The

Community Land Model version 4 (CLM4) (Oleson et al., 2010) is coupled with CAM5 to represent the evolutions of land surface boundary conditions.

Anthropogenic heating can be considered in the form of ground heat, sensible heat, or long-wave radiation (Zhang et al., 2013) in climate models, by adding the excessive vertical flux convergence in the boundary layer near the surface. Based on the physical process analysis, AHR is taken as the sensible heat flux near the surface in CAM5 in this study. Two sets of experiments are performed: one set of experiments considers the AHR in the surface energy balance within the model, while the other set of experiments does not consider the AHR as in the standard version of CAM5. Each set of experiments includes five ensemble simulations to account for the internal variability, by perturbing the initial air temperature as done by Kay et al. (2015). The simulations are initialized in January of 1992 and continue through December of 2013 (22 years), after a 5-year spin up in which all the aforementioned forcings, as well as AHR, are set in 1992. The purpose of this spin up is to eliminate the possible instability in the atmospheric and land states after the inclusion of AHR.

3. Model Results

3.1 The effect of AHR on global surface temperature

The heating effect of AHR on global annual mean surface temperature is shown as Figure 2. From the modeling results, AHR increases global mean surface temperature by about 0.02 ± 0.01 K (1σ uncertainty), and increases the global land annual surface temperature by about 0.05 ± 0.02 K (1σ uncertainty). The results show that AHR can have a significant effect on the mid- and high latitudes in the Northern Hemisphere

(NH), leading to a 0.5 K – 1 K increase in the regions between 40 ° N – 70 ° N of Eurasia. Additionally, AHR can have an obvious effect on Eastern US and Northern Africa, leading to a surface temperature increase of 0.2 K – 0.5 K. Surprisingly, a cooling effect is found in Central North America. The warming centers do not correspond to the regions where the AHR is concentrated, which can be a result of dynamical feedbacks induced by AHR. The heating effect of AHR has a significant impact on the surface energy balance: the warming centers receive more energy at the surface due to the heating effect of AHR, while the cooling centers are the regions receive less energy at the surface. The detailed feedbacks on the global lower atmosphere due to the heating effect of AHR in different seasons will be discussed below.

3.2 Climatic effects and feedbacks of AHR in boreal spring (MAM)

The effects of AHR on some key meteorological fields in the lower troposphere in boreal spring (MAM) are shown in Figures 3a-9a. The effect of AHR on global surface temperature is shown in Fig.3a. The global mean surface temperature in the boreal spring increases by 0.03 ± 0.02 K (1σ uncertainty) by the heating effect of AHR. The effect of AHR is obvious in the mid- and high latitudes of Eurasia and North America, with 0.5 K – 1.0 K increase in the surface land temperature. Fig.4a shows the heating effect of AHR on the zonal lower atmosphere at 850 hPa – 1000 hPa in the NH. Generally, the heating effect of AHR on the global lower atmosphere varies at different altitudes, and the heating effect is more distinct near the surface. There is a significant increase in zonal temperature of the lower atmosphere in the populated regions between 30° N – 75° N, with obvious updrafts in 60° N - 80° N due to the heating effect of AHR. Significant decrease in zonal temperatures occur at 75° N – 90° N, with faint downdrafts in the high latitudes near the North Pole. Overall, the non-uniform heating effect of AHR leads to obvious updrafts in the NH mid- and high latitudes. These results indicate that AHR can have a significant effect on the zonal atmospheric vertical movement, which is able to further impact global atmospheric circulation. Fig.5a shows the impact of AHR on the horizontal wind at 850 hPa. The modeling results show that AHR has a significant impact on westerly winds in the NH high latitudes. A possible reason is that AHR impacts the surface temperature in the NH mid- and high latitudes, which will affect temperature gradients and wind advection in the lower atmosphere. Fig.6a shows the impact of AHR on the global planetary boundary layer height (PBLH) in the boreal spring: it has a significant effect on the PBLH in the Eastern and middle part of US, Central Europe, and North China, with the PBLH increasing by 20 – 50 m. This result shows that AHR can impact the structure of the planetary boundary layer, in which turbulence is very important for the transport of heat and water vapor. Fig.7a shows the effect of AHR on the global lower-troposphere stability (LTS), which is defined as the difference between the potential temperature of the free troposphere (700 hPa) and the surface (LTS = $\theta_{700} - \theta_0$) (Wood and Bretherton, 2006). LTS is regarded as a measure of strength of the inversion that caps the planetary boundary layer. This inversion is correlated strongly with low cloud fraction (Wood and Bretherton, 2006), which is very important for the energy balance at the surface. The results in Fig.7a show that AHR reduces LTS on land in the boreal spring generally; AHR significantly reduces the LTS in Europe, Eastern US, and high latitudes of Eurasia, where the PBLH is increased. The probable reason is that the heating effect from AHR increases the temperature of lower atmosphere, and as a result the LTS is reduced. The results in Fig.8a show that AHR can impact the global distribution of low clouds， which is consistent with the results in Fig.7a. It reduces low clouds in mid-latitudes between 40° N – 70° N in North America, Europe and Northeast Eurasia, while it increases low clouds in the NH high latitudes. Fig. 9a shows the net shortwave flux change at the surface in the boreal spring due to the heating effect of AHR. The change in the net shortwave flux at the surface is generally consistent with the changes in low cloud fraction and global land temperature by AHR in boreal spring. For example, net shortwave flux increases in Europe and Eastern US, where low cloud fraction is reduced, indicating the reduced shortwave cloud forcing. From our results, the effect of AHR in boreal spring show that AHR heats the global lower atmosphere and affects the thermodynamic structure, LTS, and the height of planetary boundary layer, which exerts obvious impacts on global atmospheric vertical and horizontal movement, and low cloud fraction. As low clouds are important for the energy balance in the Earth-atmosphere system (IPCC, 2013), the change in net shortwave radiation at the surface due to AHR can be the possible reason for these temperature changes. Our results also indicate that global atmospheric circulation can be changed by the uneven heating effect of AHR, which are responsible for the discrepancy between the warming centers and the heating areas.

3.3 Climatic effects and feedbacks of AHR in boreal summer (JJA)

The effects of AHR on the global lower troposphere in boreal summer are shown in Figures 3b-9b. The effect of AHR on global surface temperature in the boreal summer is illustrated in Fig.3b: the global mean surface temperature in boreal summer increases by 0.02 K ±0.01 K (1σ uncertainty), while global land mean surface temperature increases by 0.06 K±0.01 K (1σ uncertainty). The surface temperature in Eastern North America, Europe, and Northeastern Eurasia has increased significantly due to the heating effect of AHR. In the selected regions (40° N – 60° N, 0° E – 45° E) in Central and Western Europe the average surface temperature increases by 0.46 K, while in Eastern North America and Northeastern Eurasia it increases by 0.2 – 0.5 K. In contrast, surface temperature decreases in the high latitudes of Central Eurasia. Fig.4b shows the heating effect of AHR on the zonal lower atmosphere at 850 hPa – 1000 hPa in NH in the boreal summer. The heating effect is not very obvious in summer overall, and is the strongest above 970 hPa between 40° N – 60° N , while the temperature near the surface shows a cooling effect generally due to the lower atmospheric movement caused by the heating of AHR. Obvious updrafts caused by AHR show in the high latitudes between 65° N – 85° N. From Fig.5b, AHR has significant impacts on the global lower atmospheric horizontal westerly wind at 850 hPa in the NH high latitudes, and on the easterly wind at 850 hPa in the high latitudes of the Southern Hemisphere (SH). The wind blowing from the seas to the continents is strengthened by the non-uniform heating effect of AHR in the boreal summer. The land surface temperature rises due to the heating effect of AHR, enhancing the surface temperature gradient between land and ocean in boreal summer. Fig.6b shows that AHR increases the PBLH in the Central US, Europe, Eastern China and Northeastern Eurasia (all of which are generally located between 30° N – 70° N) by 20 – 50 m. Fig.7b shows that the LTS in Europe decreases due to the heating effect of AHR, while in Northeastern Eurasia the LTS increases significantly. These results suggest that the clouds in Europe and Northeastern Eurasia could be affected due to the change of LTS caused by AHR, which is confirmed in Fig.8b showing the impact of AHR on low cloud fraction. The results illustrate that AHR heats the lower atmosphere, reducing LTS and the low cloud fraction in the heating regions. The low cloud is reduced by 2-4% in Europe between 30° N – 70° N and in the Arctic, while the low clouds in central part of Eurasia between 60° N – 80° N increase obviously due to the effect of AHR. Fig. 9b illustrates that the net shortwave flux decreases in the NH high latitudes in the boreal summer due to the effect of AHR. As low clouds are reduced, more shortwave radiation is reflected into space due to high surface albedo without multiple reflections between low clouds and the surface in the NH high latitudes. In addition, the energy balance at the surface is analyzed, and the change in the net shortwave flux at the surface is found to be quite consistent with the change in the global surface temperature by AHR in the boreal summer. From Fig.9b the net shortwave flux in Europe and Northeastern Eurasia increases by 3-10 W m^{-2} in the summer due to the heating effect of AHR. This shortwave flux increase corresponds to the regions where surface temperature clearly increases (Fig.3b). Meanwhile, the net shortwave flux decreases by 3-5 W m^{-2} in the high latitudes of

Central Eurasia, which agrees well with the cooling regions due to the effect of AHR. These results suggest that the change in net shortwave radiation at surface due to AHR can be the probable cause for these temperature changes. As a whole, these results suggest that AHR is able to affect the thermodynamic structure of the planetary boundary layer and LTS, as well as enhance the gradient in surface temperatures between land and ocean in boreal summer. As LTS is considered to be an important factor for low cloud fraction (Wood and Bretherton, 2006), low clouds are also changed，which is a possible feedback mechanism from the heating of the global lower atmosphere by AHR.

3.4 Climatic effects and feedbacks of AHR in boreal autumn (SON)

The effects of AHR on the global lower troposphere in boreal autumn (SON) are shown in Figures 3c-9c. The effect of AHR on global surface temperature in boreal autumn is shown in Fig.3c: The global mean surface temperature increases by 0.01 K $\pm$0.01 K (1σ uncertainty) due to the heating effect of AHR, which is statistically insignificant. However, the surface temperature in Southwestern Eurasia and Central USA increases by 0.2 – 0.5 K. A decrease in temperature by 0.5 – 1 K can be seen in Northern Europe and Northern North America. Fig.4c shows the heating effect of AHR on the zonal lower atmosphere at 850 hPa – 1000 hPa in NH in the boreal autumn: zonal temperature of the lower atmosphere increases by 0.5 – 1 K near the surface in the populated regions between 40° N – 75° N, with obvious updrafts in the NH high latitudes. Fig.5c shows the impact of AHR on the global lower atmospheric horizontal wind at 850 hPa in autumn: the wind blowing from the ocean to the continent is strengthened at the NH mid- and high latitudes. This result suggests that AHR is important for global horizontal atmospheric movement, which can further impact global atmospheric circulation. Fig.6c shows the impact of AHR on the global PBLH in the boreal autumn: AHR increases PBLH in Southeastern North America, Central Europe, Northern China, and Japan by 10 – 20 meters. Fig.7c shows that the effect of AHR on the LTS is not generally significant with slight increases between 50° N – 70° N of North America and Northern Europe. Fig.8c shows the impact of AHR on the low cloud fraction, which is consistent with the warming centers in Fig.3c. The low clouds are reduced in the high latitudes of North America and Northeastern Eurasia, corresponding to warming centers in these regions, while the low clouds are increased in central Eurasia, corresponding to the cooling centers. Fig.9c shows the change in short-wave radiation due to the effect of AHR, which is quite consistent with the changes in surface temperature and low cloud fraction. In the warming centers in central Eurasia, the net shortwave flux at the surface increases by 3-5 W m^{-2}, while in the high latitudes of North America and Europe, the net shortwave flux at the surface decreases by 3-5 W m^{-2}. These results suggest strong correlations between changes in low clouds, the net shortwave flux at the surface, and surface temperature due to the effect of AHR. These effects of AHR in boreal autumn are not distinct compared with other seasons. AHR is able to affect the thermodynamic structure and LTS, which can impact the global lower atmospheric vertical and horizontal movement, and low cloud fraction. This process is very important for the energy balance at the surface, which is essential for surface temperature.

3.5 Climatic effects and feedbacks of AHR in boreal winter (DJF)

The effects of AHR on the global lower troposphere in boreal winter are shown in Figures 3d-9d and Figure 9e. The effect of AHR on the global surface temperature in boreal winter is shown in Fig.3d: the global mean surface temperature in boreal winter increases by 0.03 ± 0.01 K (1σ uncertainty), while global mean land surface temperature increases by 0.10 ± 0.01 K (1σ uncertainty). In the selected regions (45° N – 75° N, 30° E – 140° E) in northern Eurasia the average surface temperature increases by 0.83 K. Additionally, the surface temperature in Northwestern Africa increases by 0.2 – 0.5 K. However, in central and Northern North America as well as Southeastern Eurasia the surface temperature decreases. Fig.4d shows the heating effect of AHR on the zonal lower atmosphere at 850 hPa – 1000 hPa in the NH in the boreal winter. The heating effect is stronger in winter than other seasons, with a distinct warming effect between 30° N – 65° N. Conversely the temperature in the NH high latitudes decreases due to the change in atmospheric movement caused by AHR. Strong updrafts caused by AHR show up in the high latitudes between 50° N – 80° N. From Fig.5d, AHR can have a significant impact on the global lower atmospheric horizontal winds at 850 hPa in the NH and SH high latitudes. The winds blowing from the sea to the continent is strengthened in the high latitudes of Eurasia and Northwestern Africa, while the winds from land to the sea is enhanced in Southeastern Eurasia by the heating effect of AHR. The possible mechanism is the warming effect in the NH mid- and high latitudes and the cooling effect in Southeastern Eurasia due to the effect of AHR. These results indicate that the differences in surface temperature between land and ocean in the regions where AHR has a significant effect will be enhanced in the boreal winter, which can be the possible physical mechanism for the change in global atmospheric vertical and horizontal movement. Fig.6d shows that AHR increases the PBLH in Eastern US, Northern China, and Central Eurasia by 10 – 20 meters. These results suggest that in the warming regions the turbulence and heat transport is strengthened. Fig.7d shows that LTS in the high latitudes of Central Eurasia and Northern Africa decreases due to the heating effect of AHR in boreal winter. Fig.8d shows the effect of AHR on low cloud fraction. Low clouds increase obviously in Australia and in the mid- and high latitudes of North America, corresponding to cooling centers. Conversely, low clouds are reduced in Europe, which corresponds to the warming center. Fig.9d shows the effect in net shortwave radiation flux at the surface due to AHR, and the result shows that the change is not obvious generally, especially in the mid- and high latitudes of Eurasia. Fig. 9e shows that the down-welling long-wave flux at the surface increases significantly in the mid- and high latitudes of Eurasia and Northern Africa in boreal winter due to the heating effect of AHR. The change in the down-welling long-wave flux at surface is found to be generally consistent with the change in global land temperature by AHR in boreal winter (in Fig.3d). These results show a possible mechanism for the surface temperature change in Fig.3d: the surface temperature decreases in North America and Australia are probably caused by the shortwave radiation reduction; while the increased surface temperature in mid- and high latitudes of Eurasia is caused by down-welling long-wave flux increase at the surface, likely caused by clouds. As we know, the surface in high latitudes of Eurasia is covered by snow in the boreal winter, with high surface albedo. When the clouds are increased in these regions, clouds will absorb longwave radiation, and they will radiate down-welling long-wave radiation to the surface. This will keep the surface temperature warm. These results suggest that AHR can impact the global vertical and horizontal movement, leading to the change in low cloud fraction, affecting down-welling long-wave flux at the surface in boreal winter.

4. Conclusions

The energy balance of the Earth-atmosphere system is the predominant factor in the global climate change (Hansen et al., 2005). Anthropogenic heat is a direct, external energy source to the Earth-atmosphere system impacting the energy balance of the Earth's surface as a result of global energy consumption. AHR is crucial for urban climate (IPCC, 2007). With the rapid development of global urbanization, more energy will be consumed as urban populations increase. The effect of AHR on urban regional climate will be enhanced. Because of this, AHR will have a great impact on global climate rather than on regional climate only. Global distribution of AHR and its possible climatic effect on the global lower troposphere in different seasons, as well as possible feedback mechanisms are examined in this study. The distributions of AHR show that North America, Europe, and East and South Asia are heating centers due to AHR. Our modeling results show that the climatic effect of AHR varies by season, and the effect of AHR is most prominent in the boreal winter. AHR contributes to the temperature increase in Europe in the boreal summer and is important for the strong increase in the surface temperature of the mid- and high latitudes of Eurasia in the boreal winter. Previous research has suggested that AHR will have an impact on atmospheric circulation and may lead to an apparent temperature increase in the NH mid- and high latitudes (Zhang et al., 2013; Chen et al., 2014). This study shows that the heating of AHR has an obvious effect on the energy balance at the surface. The down-welling longwave flux at surface is increased significantly in the NH mid- and high latitudes in the boreal winter, which is closely correlated with the increase of low clouds caused by the heating effect of AHR.

The different heating effects of AHR at various altitudes will affect the vertical motion of the lower atmosphere, which will influence the heat flux and water vapor transport in the lower atmosphere. The heating effect of AHR on the boundary layer in the concentrated regions is very important for urban regional climate. Also, the heating effect of AHR will raise the PBLH, which has an impact on the LTS of the regional atmosphere (Lin et al., 2008). AHR also affects the differences in surface temperature between land and ocean. These changes impact the atmospheric vertical and horizontal motions and global atmospheric circulation as well. Additionally, the possible climate feedback due to the heating of AHR is analyzed in each season. From our modeling results of the energy balance at the surface in boreal summer and winter, we find that the shortwave radiation flux in summer and down-welling long-wave flux at surface in winter both change significantly. As low level clouds are a dominant factor in shortwave radiation flux in summer and down-welling long-wave flux at surface in winter, the obvious effect of AHR on the LTS leads to the change in low cloud fraction, which further exerts feedbacks on the surface energy balance and surface temperature.

5. Discussion

The possible mechanism and climatic feedback due to AHR in the NH mid- and high latitudes are discussed in this study. Six groups of experiments are conducted in CAM5 in order to account for the internal variability. However, limitations exist in this research. The anthropogenic heat could be in the form of ground heat flux, sensible heat flux, or long-wave radiation (Zhang et al., 2013). The proper proportion among ground heat flux, sensible heat flux and long-wave radiation for the parameterization of AHR in climate models is still uncertain at present. In this study, we consider AHR as the sensible heat into the CAM5 model, which is consistent with Zhang et al. (2013). This differs from our previous research, which considered AHR as long-wave radiation (Chen et al., 2014). The possible difference in climate modeling results due to the different parameterizations of AHR will be discussed in more details in future studies. Additionally, our modeling results indicate that the uneven heating effect of AHR can have a significant impact on low clouds in Europe in the boreal summer, and a strong effect on low clouds in the boreal winter. According to the latest research results, low clouds are correlated with high surface temperature (Rachel et al., 2018). Considering the uncertain and complicated processes of clouds (IPCC, 2013), it is very hard to attribute the effect of AHR on clouds from climate modeling results and observations. Further research will be needed to explore the possible mechanism of AHR on the global climate change.

In a comparison used by Chen et al. (2016), GHGs emissions can be regarded as a blanket that covers the Earth. Increasing the concentration of GHGs causes this blanket to become thicker, leading to a warmer climate. In this analogy, AHR resembles an electric blanket that unevenly heats the lower atmosphere (Chen et al., 2016). The results of our study demonstrate the climatic effect of AHR on the global scale by acknowledging its role in altering the stability of the global lower troposphere and the height of the planetary boundary layer through its unevenly distributed heating, which affect the global low cloud fraction. These results indicate that AHR is an important factor for long-term global climate change, which should receive more attentions in the future climate change researches.

Acknowledgments

This work was supported by the National Natural Science Foundation of China (Grant NO. 41505126 and NO. 41865001), the Program for key Laboratory in University of Yunnan Province, and Open Project of the Ministry of Education Key Laboratory for Earth System Modeling of Tsinghua University in 2017.

References

Abdul-Razzak, H., and S. J. Ghan, 2000: A parameterization of aerosol activation: 2. Multiple aerosol types, J. Geophys. Res., 105(D5), 6837–6844, doi: 10.1029/1999JD901161.

Allen, L., Lindberg F. and Grimmond C., 2011: Global to city scale urban anthropogenic heat flux: model and variability. Int. J. of Climatol., **31**(13), 1990-2005.

Bacmeister, J. T., M. F. Wehner, R. B. Neale, A. Gettelman, C. Hannay, P. H. Lauritzen, J. M. Caron, and J. E. Truesdale, 2014: Exploratory high-resolution climate simulations using the Community Atmosphere Model (CAM). *J. Climate*, **27**, 3073-3099.

Bretherton, C. S., and Park S., 2009: A New Moist Turbulence Parameterization in the Community Atmosphere Model, J. Climate, 22, 3422-3448.

Block, A., Keuler K. and Schaller E., 2004: Impacts of anthropogenic heat on regional climate patterns, *Geophys. Res. Lett.* **31**, L 12211, doi: 10.1029/2004GL019852.

BP, 2013: Energy Outlook 2030 (available at http://www.bp.com/).

BP, 2014: British Petroleum BP Statistical Review of World Energy 2014 (available at http:// www.bp.com/statisticalreview).

Chaison, E. J., 2008: Long-term global heating from energy usage.EOS.**89**, 253-260.

Chen, B. and Shi G. Y., 2012: Estimation of the distribution of global anthropogenic heat flux, *Atmos. Oceanic. Sci. Lett.* **5**, 108-112, doi: 10.1080/16742834.2012.11446974.

——, Dong L., Liu X., Shi G.Y., Chen L., Nakajima T., Habib A., 2016: Exploring the possible effect of anthropogenic heat release due to global energy consumption upon global climate: a climate model study. *Int. J. Climatol.* **36**: 4790–4796, doi: 10.1002/joc.4669.

——, Dong L., Shi G. Y., Li L., and Chen L., 2014: Anthropogenic Heat Release: Estimation of global distribution and possible climate effect, J. Metero. Soci. Japan, **92**A, 157-165.

——, Shi G. Y., WANG B., Tan S., and Zhao J. Q., 2012: Estimation of anthropogenic heat release distribution of China from 1992 to 2009, *Acta Metero.Sinica.***26**(4), 507-515.

——, Zhao J. Q., Chen L., Shi G. Y., 2015: Reply to the Comments of F. Fujibe on "Anthropogenic Heat Release: Estimation of Global Distribution and Possible Climate Effect" by Chen, B. et al., J. Metero. Soci. Japan, **93**(4), 505-508.

Crutzen, P. J., 2004: New directions: the growing urban heat and pollution "island" effect - impact on chemistry and climate. Atmos. Environ., **38**, 3539-3540.

Dong Y., A.C.G. Varquez, M. Kanda, 2017: Global anthropogenic heat flux database with high spatial resolution, Atmos. Environ., **150**, 276-294.

Elvidge, C. D., K. E. Baugh, E. A. Kihn, Kroehl H. W., Davis E. R., and Davis C., 1997: Relation between satellite observed visible-near infrared emissions, population, economic activity and electric power consumption, *Int. J. Remote Sens.*, **18**, 1373–1379.

Fan, H. and Sailor D. J., 2005: Modeling the impacts of anthropogenic heating on the urban climate of Philadelphia: a comparison of implementations in two PBL schemes, *Atmos.Environ.***39**，73-84.

Feng, J. M., Wang Y., Ma Z., and Liu Y., 2012: Simulating the regional impacts of urbanization and anthropogenic heat release on climate across China, *J. Clim.***25**, 7187-7203.

Flanner, M. G., 2009: Integrating anthropogenic heat flux with global climate models, *Geophy.Res.Let.*36, L02801, doi: 10.1029/2008GL036465.

Gates, W. L., 1992: AMIP: The Atmospheric Model Intercomparison Project. Bull. Amer. Meteor. Soc., 73, 1962–1970.

Gettelman, A., Liu, X., Ghan, S. J., Morrison, H., Park, S., Conley, A. J., Klein, S. A., Boyle, J., Mitchell, D. L., and Li, J. L. F., 2010: Global simulations of ice nucleation and ice supersaturation with an improved cloud scheme in the Community Atmosphere Model, Journal of Geophysical Research: Atmospheres, 115, D18216, doi: 10.1029/2009JD013797.

Ghosh, T., A. Sharolyn, L. P. Rebecca, P. C. Sutton, and C. D. Elvidge, 2009: Estimation of Mexico's informal economy and remittances using nighttime imagery, *Remote Sens.*, **1**, 418–444.

Hansen, J., Nazarenko L., Reudy R., Sato M., Willis J. and coauthors, 2005: Earth's energy imbalance: Confirmation and Implications, Science, **39**, 1431-1434.

Hurrell, J. W., Holland M. M., Gent P. R., Ghan S., Kay J. E., Kushner P. J., Lamarque J. F., Large W. G., Lawrence D., Lindsay K., Lipscomb W. H., Long M. C., Mahowald N., Marsh D. R., Neale R. B., Rasch P., Vavrus S., Vertenstein M., Bader D., Collins W. D., Hack J. J., Kiehl J., and Marshall, S., 2013: The Community Earth System Model: A Framework for Collaborative Research, Bulletin of the American Meteorological Society, **94**, 1339-1360.

Iacono, M. J., Delamere J. S., Mlawer E. J., Shephard M. W., Clough S. A., and Collins W. D., 2008: Radiative forcing by long-lived greenhouse gases: Calculations with the AER radiative transfer models, Journal of Geophysical Research: Atmospheres, 113, D13103, doi: 10.1029/2008JD009944.

Ichinose, T., Shimodozono K. and Hanaki K., 1999: Impact of anthropogenic heat on urban climate in Tokyo, Atmos. *Environ.*, **33**, 3897–3909.

IPCC, 2007: *Climate change 2007*: *The Physical Science Basis. Contribution of Working Group I to the Fourth Assessment Report of the Intergovernmental Panel on Climate Change*. Solomon, S., D. Qin, M. Manning, Z. Chen, M. Marquis, K. B. Averyt, M. Tignor, and H. L. Miller (eds.), Cambridge University Press, Cambridge, UK and NY, USA.

IPCC, 2013: *Climate Change 2013*. The Physical Science Basis. Contribution of Working Group I to the Fifth Assessment Report of the Intergovernmental Panel on Climate Change [Stocker, T.F., D. Qin, G.-K. Plattner, et al.,(eds.)]. Cambridge University Press, Cambridge, United Kingdom and New York, NY, USA.

Kay, J. E., Deser C., Phillips A., Mai A., Hannay C., Strand G., Arblaster J., Bates S., Danabasoglu G., Edwards J., Holland M. Kushner P., Lamarque J.-F., Lawrence D., Lindsay K., Middleton A., Munoz E., Neale R., Oleson K., Polvani L., and M. Vertenstein, 2015: The Community Earth System Model (CESM) Large Ensemble

Project: A Community Resource for Studying Climate Change in the Presence of Internal Climate Variability, Bulletin of the American Meteorological Society, 1, 96, 1333-1349.

Lee, S. H., Song C. K., Baik J. J., and Park S. U., 2009: Estimation of anthropogenic heat emission in the Gyeong-In region of Korea, *Theor. Appl.Climatol*. **96**, 291-303.

Li, L. J., Wang B., Dong L., Liu L., Shen S. and coauthors, 2013: Evaluation of Grid-Point Atmospheric Model of IAP LASG version2 (GAMIL 2). *Adv.Atmos.Sci.,* **30**(3), 855-867.

Lin, C. Y., F. Chen, J. C. Huang, W. C. Chen, Y. A. Liou, W. N. Chen, and S. C. Liu, 2008: Urban heat island effect and its impact on boundary layer development and land– sea circulation over northern Taiwan, Atmos. Environ., **42**, 5635-5649, doi:10.1016/j.atmosenv.2008.03.015.

Lindberg, F., Grimmond C., Yogeswaran N., Kotthaus S. and Allen L., 2013: Impact of city changes and weather on anthropogenic heat flux in Europe 1995–2015, Urban Climate, **4**, 1-15.

Liu, X., Easter R. C., Ghan S. J., Zaveri R., Rasch P., Shi X., Lamarque J. F., Gettelman A., Morrison H., Vitt F., Conley A., Park S., Neale R., Hannay C., Ekman A. M. L., Hess P., Mahowald N., Collins W., Iacono M. J., Bretherton C. S., Flanner M. G., and Mitchell D., 2012: Toward a minimal representation of aerosols in climate models: description and evaluation in the Community Atmosphere Model CAM5, Geosci. Model Dev., 5, 709-739.

Liu X. and J. E. Penner, 2005: Ice nucleation parameterization for global models, Meteorologische Zeitschrift, 14, No.4, 499-514.

Liu X., J. E. Penner, S. J. Ghan, and M. Wang, 2007: Inclusion of Ice Microphysics in the NCAR Community Atmospheric Model Version 3 (CAM3), Journal of Climate, **20**, 4526-4547.

McCarthy, M. P., Best M. J. and Betts R. A., 2010: Climate change in cities due to global warming and urban effect, *Geophys.Res.Lett.*, **37**, L09705, doi: 10.129/2010GL042845.

Morrison, H., and Gettelman A., 2008: A New Two-Moment Bulk Stratiform Cloud Microphysics Scheme in the Community Atmosphere Model, Version 3 (CAM3). Part I: Description and Numerical Tests, J Climate, **21**, 3642-3659.

Neale, R. B., and Coauthors., 2010: Description of the NCAR Community Atmosphere Model (CAM5.0). NCAR Tech. Rep. NCAR/ TN-4861STR, 274pp.

Oke, T. R., 1988: The urban energy balance. Progress in Physical Geography, 12, 471–580.

Oleson, K. W., Bonan G. B., Fedema J. and Jackson T., 2011: An examination of urban heat island characteristics in a global climate model, *Int.J.Climatol.*, **31**(12), 1848-1865.

——, Lawrence D. M., Gordon B., Flanner M. G., Kluzek E., Peter J., Levis S., Swenson S. C., Thornton E., and Feddema J., 2010: Technical description of version 4.0 of the Community Land Model (CLM), NCAR Tech. Note NCAR/TN-461+STR.

Park, S., and Bretherton C. S., 2009: The University of Washington Shallow Convection and Moist Turbulence Schemes and Their Impact on Climate Simulations with the Community Atmosphere Model, J. Climate, **22**, 3449-3469.

——, Bretherton C. S., and Rasch P. J. 2014: Integrating Cloud Processes in the Community Atmosphere Model, Version 5, J. Climate, **27**, 6821-6856.

Rachel E. S. Clemesha, K. Guirguis, A. Gershunov, I. J. Small, A. Tardy, 2018: California heat waves: their spatial evolution, variation, and coastal modulation by low clouds, Clim. Dyn., **50**, 4285–4301.

Richter, J. H., and Rasch P. J., 2008: Effects of Convective Momentum Transport on the Atmospheric Circulation in the Community Atmosphere Model, Version 3, J. Climate, **21**, 1487-1499.

Sailor, D. J. and Lu L., 2004: A top-down methodology for developing diurnal and seasonal anthropogenic heating profiles for urban areas, *Atmos. Environ*., **38**, 2737-2748.

Wang, X., Sun, X., Tang, J., and Yang, X., 2015: Urbanization-induced regional warming in Yangtze River Delta: potential role of anthropogenic heat release, *Int. J. Climatol.,* **35**(15), 4417-4430.

Wood, R., and Bretherton C.S., 2006: On the Relationship between Stratiform Low Cloud Cover and Lower-Tropospheric Stability, J. Climate, **19**, 6425–6432.

Wu, K. and Yang X., 2013: Urbanization and heterogeneous surface warming in eastern China. Chin. Sci. Bull., **58**: 1363□1373.

Yang W., Jiang C., Yu X., et al, 2014: Review of research on anthropogenic heat under climate change, Progress in Geography, **33**(8): 1029-1038.

Zhang, G. J., Cai M. and Hu A., 2013: Energy consumption and the unexplained winter warming over northern Asia and North America, *Nature climate change*. **3**,466-470.

——, and McFarlane N. A., 1995: Sensitivity of climate simulations to the parameterization of cumulus convection in the Canadian Climate Centre general circulation model, Atmosphere-Ocean, **33**, 407-446.

Zhong, S., Qian Y., Zhao C., Leung R., Wang H., Yang B., Fan J., Yan H., Yang X.Q., and Liu D., 2017: Urbanization-induced urban heat island and aerosol effects on climate extremes in the Yangtze River Delta region of China, Atmos. Chem. Phys., **17**, 5439-5457.

1. Figure 1

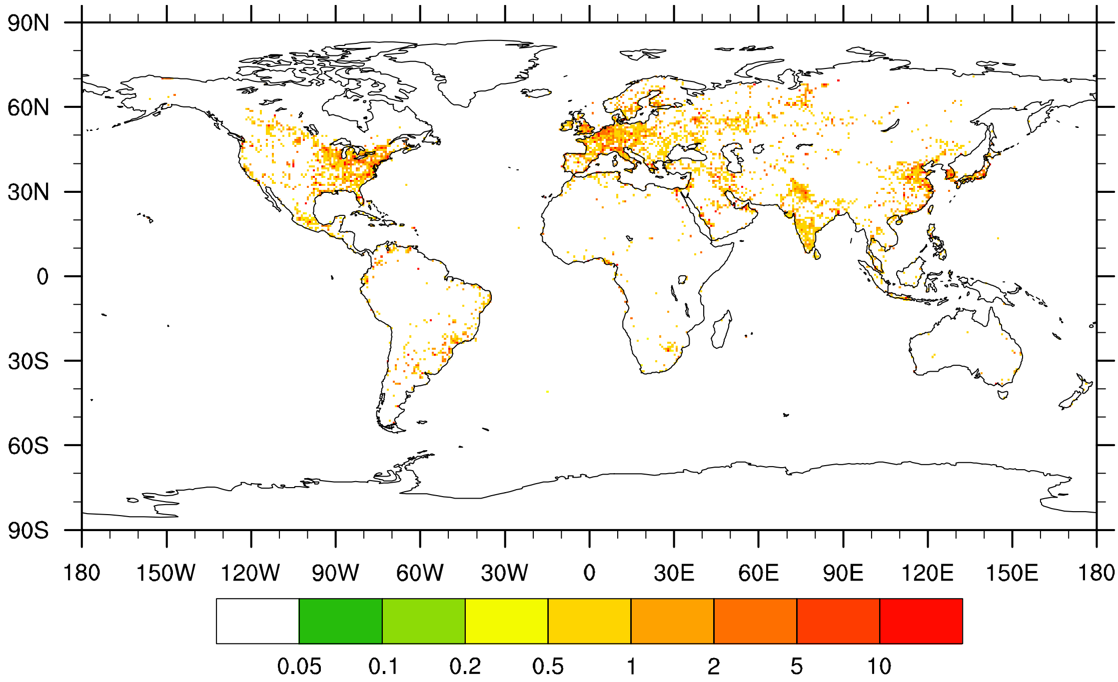

Fig.1 Estimation of the distribution of global AHR in the year 2013 (resolution: 0.1° × 0.1°; unit: W m^{-2}).

2. Figure 2

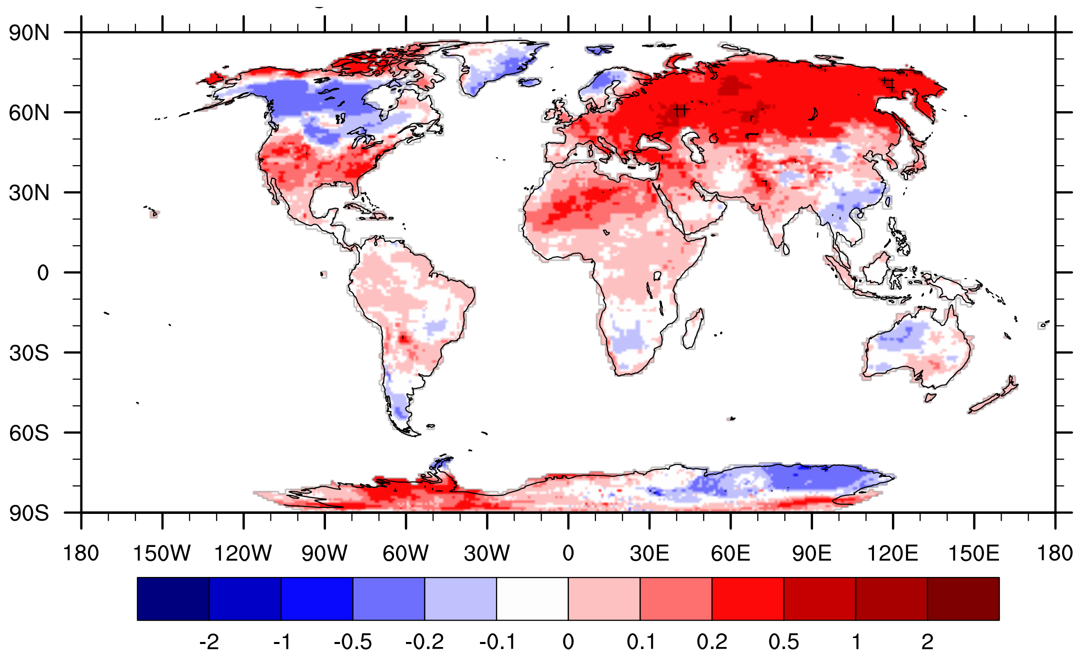

Fig.2 Effect of AHR on global land mean surface temperature, unit: K. (The plus signs in Figure 2 denote the change is statistically significant at the 0.10 level.)

3. Figure 3

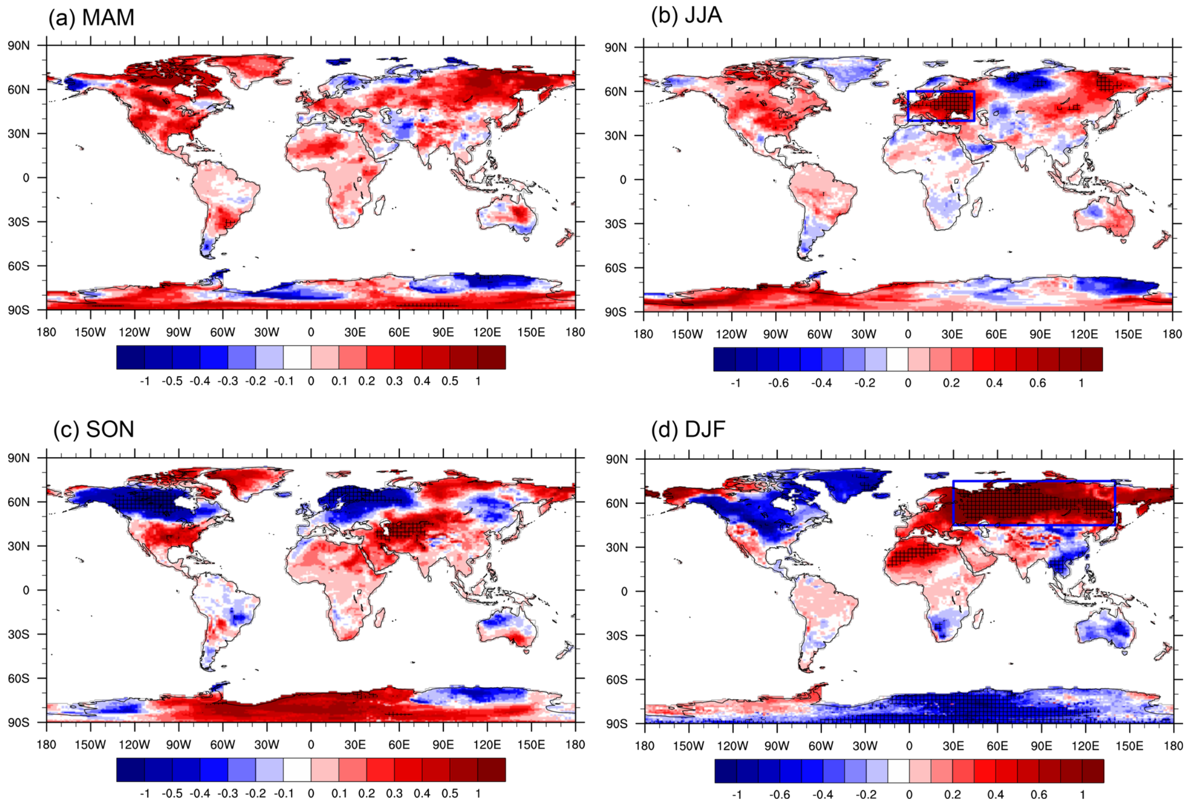

Fig.3 The effects of AHR on global land mean surface temperature (unit: K): (a) in boreal spring (MAM); (b) in boreal summer (JJA); (c) in boreal autumn (SON); and (d) in boreal winter (DJF). The plus signs in Fig. 3 denote the change is statistically significant at the 0.10 level.

4. Figure 4

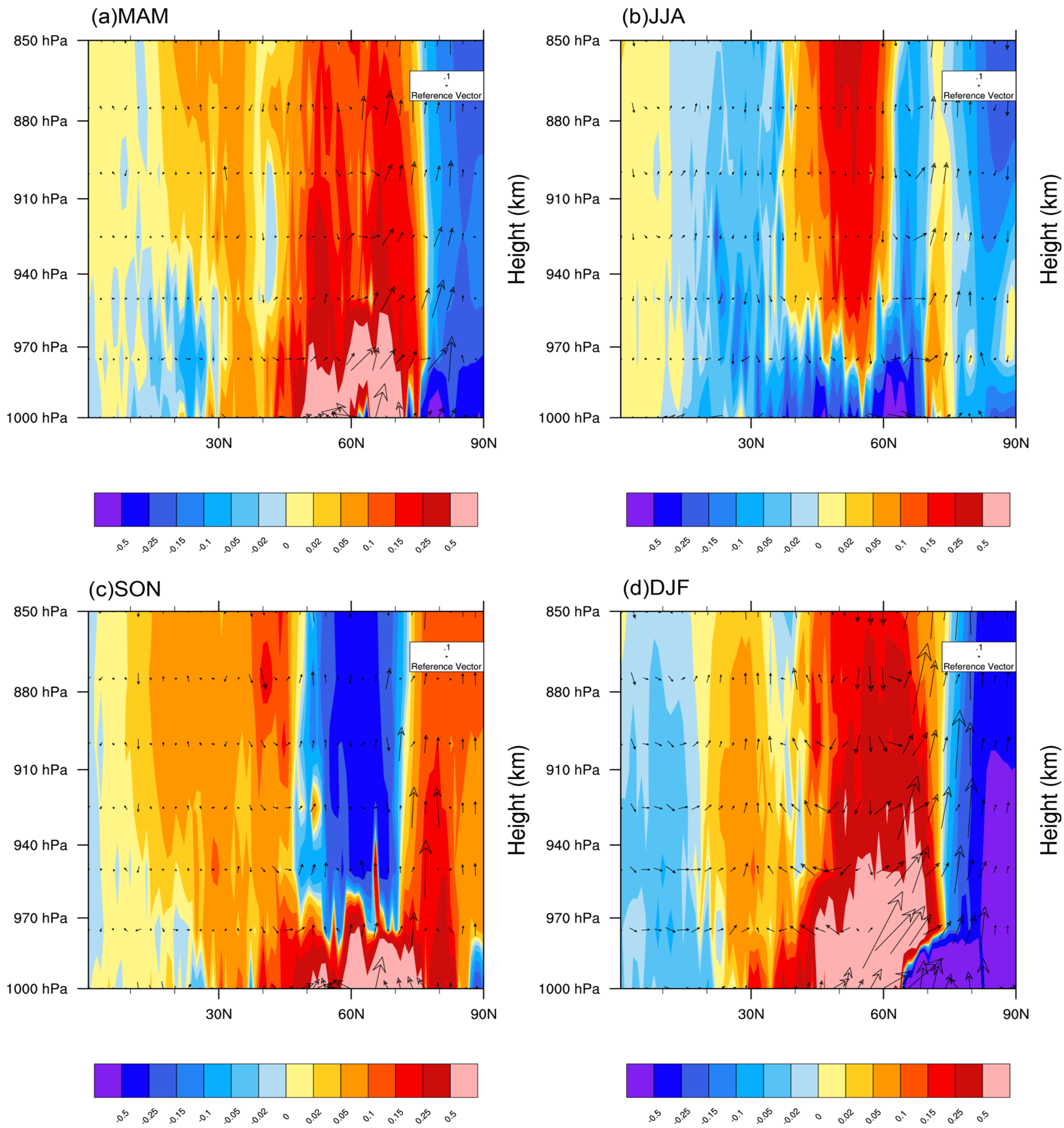

Fig.4 The effects of AHR on height-latitude cross-section of differences in temperature (shaded in K) and vertical circulation (vectors, meridional wind in 0.1 m s^{-1} and vertical velocity in -0.01 Pa s^{-1}) averaged over North Hemisphere: (a) in boreal spring (MAM); (b) in boreal summer (JJA); (c) in boreal autumn (SON); and (d) in boreal winter (DJF). The plus signs in Fig. 4 denote the change is statistically significant at the 0.10 level.

5. Figure 5

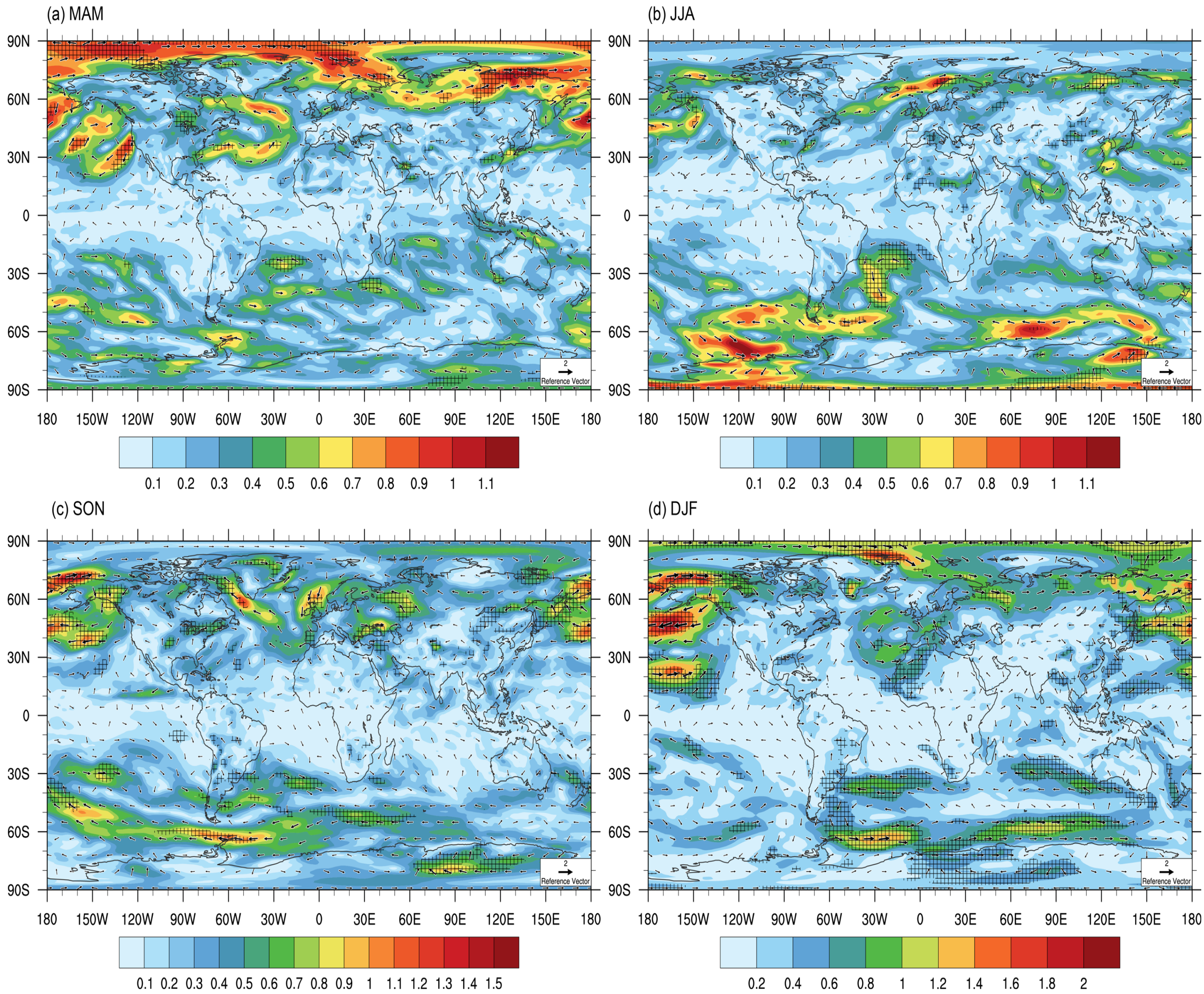

Fig.5 The effects of AHR on horizontal wind (U, V) at 850 hPa (unit: m s^{-1}): (a) in boreal spring (MAM); (b) in boreal summer (JJA); (c) in boreal autumn (SON); and (d) in boreal winter (DJF). The plus signs in Fig. 5 denote the change is statistically significant at the 0.10 level.

6. Figure 6

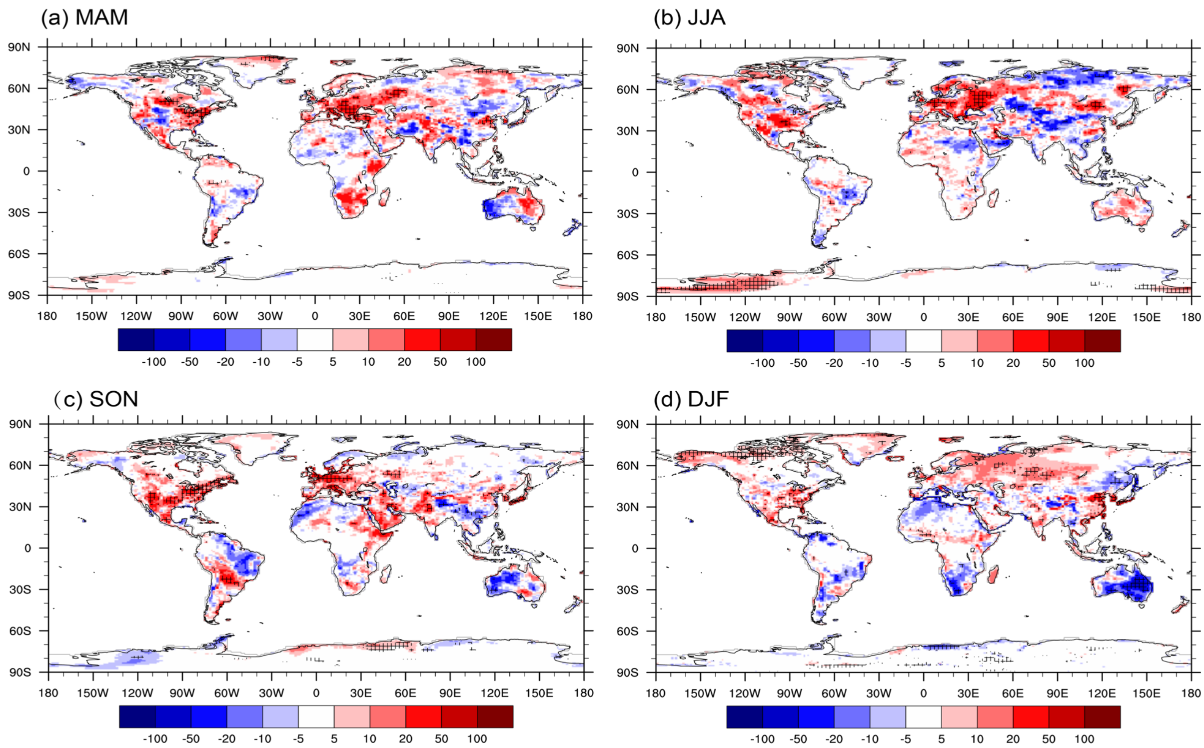

Fig.6 The effects of AHR on the planetary boundary layer height (PBLH, unit: m): (a) in boreal spring (MAM); (b) in boreal summer (JJA); (c) in boreal autumn (SON); and (d) in boreal winter (DJF). The plus signs in Fig. 6 denote the change is statistically significant at the 0.10 level.

7. Figure 7

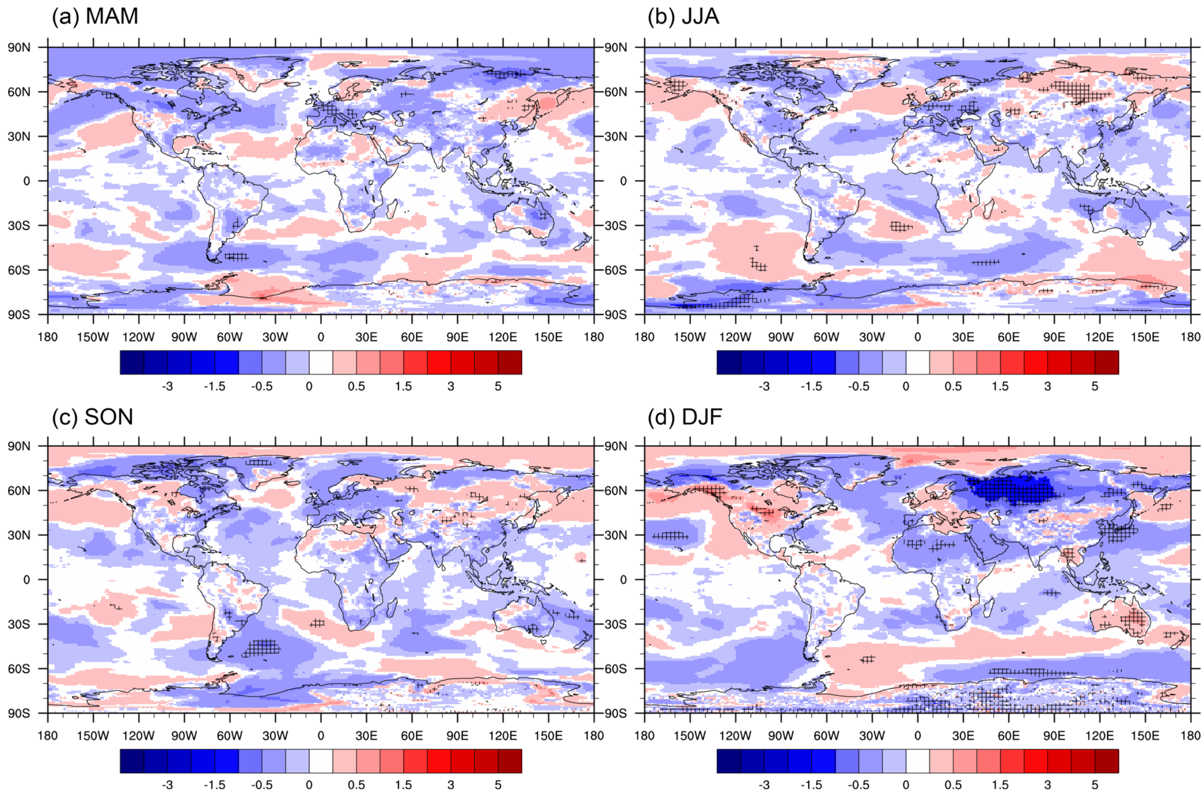

Fig.7 The effects of AHR on the lower-troposphere stability (LTS, unit: K): (a) in boreal spring (MAM); (b) in boreal summer (JJA); (c) in boreal autumn (SON); and (d) in boreal winter (DJF). The plus signs in Fig. 7 denote the change is statistically significant at the 0.10 level.

8. Figure 8

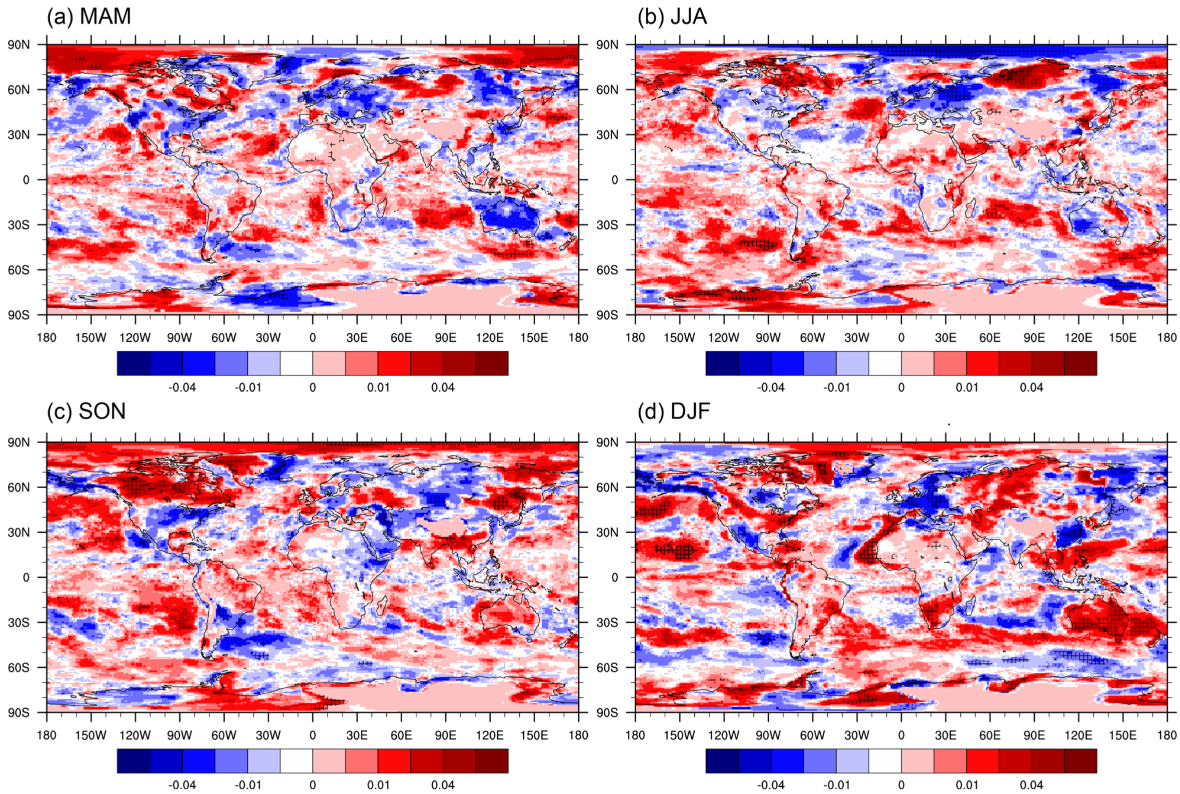

Fig.8 The effects of AHR on the low cloud fraction: (a) in boreal spring (MAM); (b) in boreal summer (JJA); (c) in boreal autumn (SON); and (d) in boreal winter (DJF). The plus signs in Fig. 8 denote the change is statistically significant at the 0.10 level.

9. Figure 9

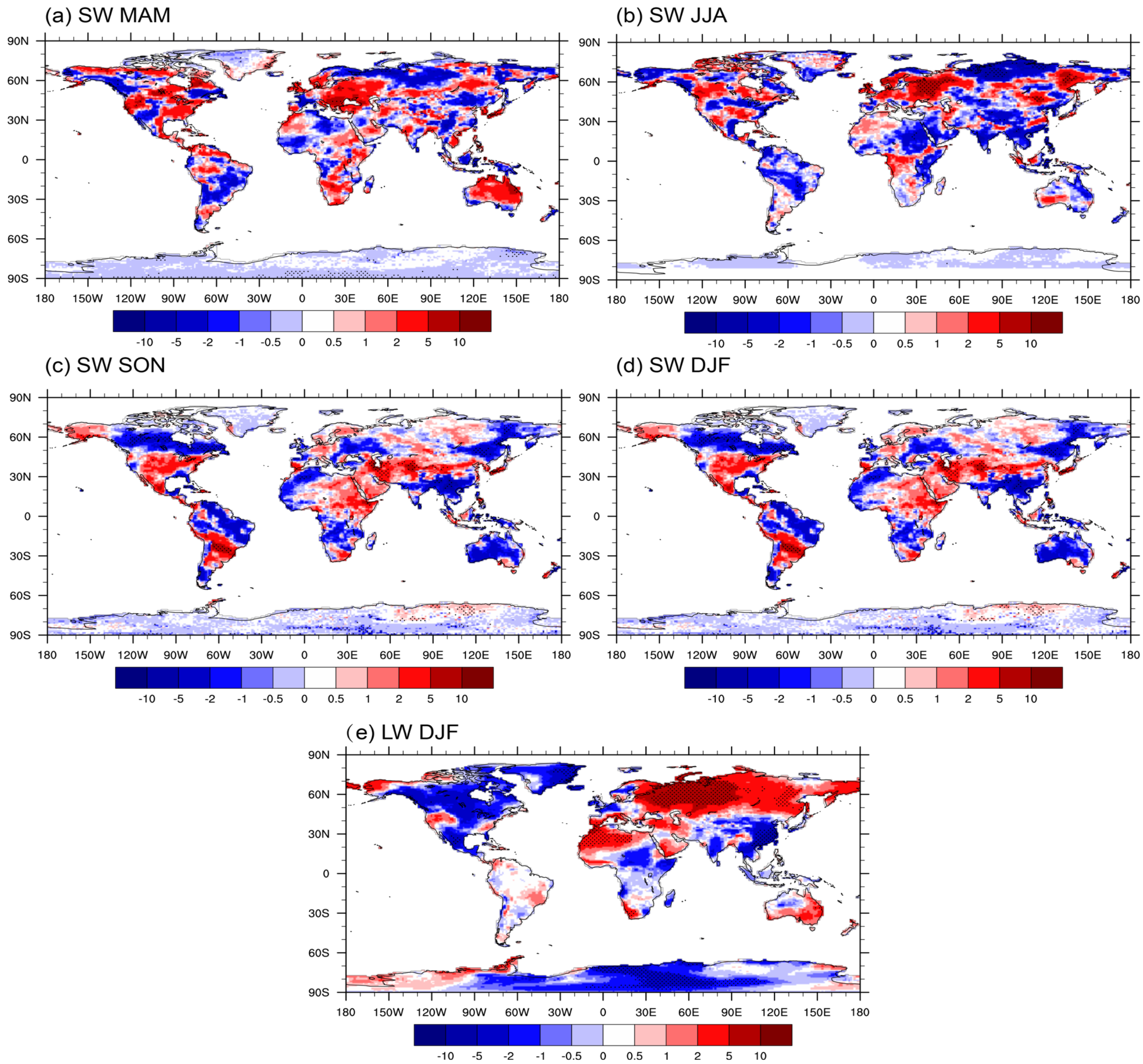

Fig.9 The effects of AHR on the energy balance at the surface (unit: W m^{-2}): (a) the net shortwave flux at the surface in boreal spring (MAM); (b) the net shortwave flux at the surface in boreal summer (JJA); (c) the net shortwave flux at the surface in boreal autumn (SON); (d) the net shortwave flux at the surface in boreal winter (DJF); and (e) the downwelling longwave flux at surface in boreal winter (DJF). The plus signs in Fig. 9 denote the change is statistically significant at the 0.10 level.